Angular momentum quantum backflow in the noncommutative plane

Valentin Daniel Paccoia,[1,*] Orlando Panella ®,[2,†] and Pinaki Roy ®[3,4,‡]

[1]*Dipartimento di Fisica e Geologia, Università degli Studi di Perugia, Via A. Pascoli, 06123, Perugia, Italy*
[2]*Istituto Nazionale di Fisica Nucleare, Sezione di Perugia, Via A. Pascoli, I-06123 Perugia, Italy*
[3]*Atomic Molecular and Optical Physics Research Group, Advanced Institute of Materials Science,*
Ton Duc Thang University, Ho Chi Minh City, Vietnam
[4]*Faculty of Applied Sciences, Ton Duc Thang University, Ho Chi Minh City, Vietnam*

We study the quantum backflow problem in the noncommutative plane. In particular, we have considered a charged particle with and without an oscillator interaction with noncommuting momentum operators and examined angular momentum backflow in each case and how they differ from each other. We also propose a probability associated with the occurrence of angular momentum backflow and investigate whether or not the probability depends on a physical parameter, namely, the magnetic field.

I. INTRODUCTION

Quantum backflow is a striking but still relatively not well-known quantum effect for which, given a state containing only positive momentum components, the probability of observing the particle to the right of a given reference point ($x = 0$ for instance), may actually decrease over time. This amounts to saying that there is a flow of the probability density in the direction opposite to that of the momentum. In other words, it means that a right-moving particle can actually move to the left. The effect was first discovered by Allcock in his works on arrival time, and it was noted that the probability current could be negative for states consisting only of positive momenta [1–3].

A detailed investigation of the problem was carried out and an upper bound to the amount of probability that can flow in a direction opposite to momentum was found [4]. This limit c_{bm} has a numerically computed value of about 0.04 and the most surprising fact is that it is a dimensionless value, independent of any physical parameter. Because of that it has been considered as "a new quantum number." This may cause some problems in the naive classical limit $\hbar \to 0$ as it has been observed how there are different systems for which the maximum amount of backflow becomes dependent on some physical parameters. However, it has been shown [5], in a one-dimensional setting, that with a more realistic approach introducing quasiprojectors[1] $\theta_\sigma(\hat{x})$ of the position operator smoothed, over a length scale σ, instead of the ideal projector $\theta(\hat{x})$, the limit $\hbar \to 0$ reproduces correctly the

classical behavior, i.e., no backflow. On the other hand, in the case of a Dirac particle backflow was found to depend on some physical parameters [6,7] but not in a way that explains the classical limit. See also [8,9] for a discussion of the quantum backflow in the Dirac equation of spin-$\frac{1}{2}$ free particles.

There have been attempts to improve the value c_{bm} [10,11]. In particular, in [11] an operator associated with the backflow problem was found and was used to improve upon the value of c_{bm}. However, although the problem of finding the exact eigenstate corresponding to the upper bound of c_{bm} (maximum backflow) has still not been solved analytically, there are plenty of constructions of backflowing states.

In an interesting approach [12], the backflow problem was studied using non-normalizable wave functions and it was found that in relation to the superoscillations a constraint regarding spatial extension exists. By measuring the fraction of the x axis subject to backflow, the probability of finding the particle in one one these regions, and their temporal evolution, was found. Interestingly, quantum backflow has also been studied in different contexts like decay of metastable states [13], in multiparticle systems [14], appearance of classically forbidden probability flux [15], etc. In another recent work [16] the author discusses the relationship between quantum backflow and quantum reentry (QR), the effect in which a wave packet evolving from a localized spatial region partially returns to this region in the absence of external forces, providing a unifying treatment of the two effects.

It may be noted that in interacting systems, the backflow problem can be studied in different ways. For example, quantum backflow has been studied in the context of scattering states in Ref. [17] where it has been shown that those features of the probability operator in the quantum backflow in the case of no interactions are also found when interactions are present. The most important properties of the quantum backflow are

---

*valentindaniel.paccoia@studenti.unipg.it
†Corresponding author: orlando.panella@pg.infn.it
‡pinaki.roy@tdtu.edu.vn

[1]The smoothed quasiprojector $\theta_\sigma(\hat{x}) = \int_0^\infty dy\, \delta_\sigma(\hat{x} - y)$ is defined in terms of a smoothed (over a length scale σ) Dirac δ : $\delta_\sigma(\hat{x} - y) = \frac{1}{\sqrt{2\pi\sigma^2}} \exp\left[-\frac{(\hat{x}-y)^2}{\sigma^2}\right]$.

stable against the introduction of interaction potentials, even strong ones.

In another example [18,19], considering an electron in a magnetic field, the backflow problem has been formulated in terms of an effective angular momentum defined for states given as a superposition of eigenstates and written out the in phase-amplitude form. It was shown [18] that in certain regions of space the effective angular momentum can be directed in a direction opposite to that of the wave function's components. These results are very interesting since they show that while the usual momentum quantum backflow is related to the uncertainty relation between the position coordinate and the momentum [18], the angular momentum backflow relates to the uncertainty relations between the polar (azimuthal) coordinate and the z-component of the canonical angular momentum operator (L_z^{can}). This could mean that similar effects could be found for other models where additional interactions are present.

During the past decade or so, studies on quantum gravity and string theory indicate that space may be noncommutative in nature [20–22]. In order to test the effect of space noncommutativity several quantum mechanical models, e.g., harmonic oscillator [23–25], central field problems [26,27], hydrogen problem [28,29], etc., have been studied within the framework of noncommutative quantum mechanics. In all these cases attempts were made to determine the effect of noncommutativity by finding the dependence of some observable like energy on the parameter(s) of noncommutativity. In some other cases the effect of noncommutativity on phenomena like chirality phase transition [30], Hall effect in Dirac matter like graphene [31–33], etc., have been studied. However, in view of the fact that no conclusive evidence regarding noncommutative nature of space or momenta has yet been conclusively established, it is of interest to find new models where this effect may eventually be detected. In this context, it may be noted that in recent years experiments have been proposed to detect quantum backflow in Bose-Einstein condensate [34] as well as in the field of optics [35].

In this paper our objective is to study the quantum backflow problem on the the noncommutative plane. To be more specific, we shall consider two models: (1) The first one is a noncommutative analog of a charged particle in the presence of a homogeneous magnetic field. (2) A noncommutative oscillator in a homogeneous magnetic field. In both the models we shall study angular momentum backflow [18] and examine to what extent the noncommuting nature of the momentum operators affects quantum backflow. In this context it may be noted that the second model is a more general one from which the first one can be obtained by setting the oscillator frequency equal to zero. Nevertheless, we have treated them separately as the first one has a commutative analog [18] with which we may compare our results and the second one has no counterpart. Second, it also helps us to find out the difference in backflow pattern when an additional interaction is present. Finally, we shall also make an attempt to quantify angular momentum backflow by defining a suitable probability associated with it. The organization of the paper is as follows: In Sec. II we formulate the model(s) on the noncommutative plane and obtain the solutions; in Sec. III we study angular momentum backflow in a noncommutative setting; in Sec. IV we define a

probability associated with angular momentum backflow and discuss some of its features; finally, Sec. V is devoted to the conclusions.

II. NONCOMMUTATIVE CHARGED PARTICLE SUBJECT TO AN OSCILLATOR IN A MAGNETIC FIELD

To begin with, we note that the Hamiltonian H_{NC} for a particle of charge q in the noncommutative plane in the presence of a homogeneous magnetic field subject to an oscillator potential has the same functional form as the one in the commutative plane. Thus, the Hamiltonian H_{NC} is taken to be of the form

$$H_{\mathrm{NC}} = \frac{1}{2\mu}\left(\hat{\boldsymbol{p}} - \frac{q}{c}\hat{\boldsymbol{A}}\right)^2 + \frac{1}{2}\mu\omega^2(\hat{x}^2 + \hat{y}^2), \qquad (1)$$

where c is the velocity of light, and μ is the particle's mass. We choose the vector potential to be analogous to the one in the commutative plane producing a constant magnetic field along the z axis as $\boldsymbol{B} = B\hat{\boldsymbol{k}}$, $\hat{\boldsymbol{k}}$ being the z-axis unit vector:

$$\hat{\boldsymbol{A}} = (-B\hat{y}/2, B\hat{x}/2). \qquad (2)$$

The commutation relations between the noncommuting coordinates and momenta are given by [36]

$$[\hat{x}, \hat{y}] = i\theta, \qquad\qquad [\hat{p}_x, \hat{p}_y] = i\eta,$$
$$[\hat{x}_i, \hat{p}_j] = i\hbar\left(1 + \frac{\theta\eta}{4\hbar^2}\right)\delta_{ij}, \qquad \theta, \eta \in \mathbb{R}. \qquad (3)$$

Then for an electron, charge $q = -e$, the above noncommutative Hamiltonian reads as

$$H_{\mathrm{NC}} = \frac{1}{2\mu}\left(\hat{p}_x - \frac{eB}{2c}\hat{y}, \hat{p}_y + \frac{eB}{2c}\hat{x}\right)^2 + \frac{1}{2}\mu\omega^2(\hat{x}^2 + \hat{y}^2). \quad (4)$$

Using the commutation relations in Eq. (3) we obtain

$$\left(\hat{p}_x - \frac{eB}{2c}\hat{y}\right)^2 = \hat{p}_x^2 + \left(\frac{eB}{2c}\right)^2\hat{y}^2 - \frac{eB}{c}\hat{y}\hat{p}_x, \qquad (5)$$

$$\left(\hat{p}_y + \frac{eB}{2c}\hat{x}\right)^2 = \hat{p}_y^2 + \left(\frac{eB}{2c}\right)^2\hat{x}^2 + \frac{eB}{c}\hat{x}\hat{p}_y. \qquad (6)$$

It is now necessary to express the noncommuting coordinates and momenta in terms of commuting ones. This can be achieved using the Seiberg-Witten map [37] and the transformations are given by

$$\hat{x} = x - \frac{\theta}{2\hbar}p_y, \quad \hat{p}_x = p_x + \frac{\eta}{2\hbar}y,$$
$$\hat{y} = y + \frac{\theta}{2\hbar}p_x, \quad \hat{p}_y = p_y - \frac{\eta}{2\hbar}x, \qquad (7)$$

where (x, y) and (p_x, p_y) denote commuting coordinates and momenta. Now using the relations in Eq. (7) the Hamiltonian in Eq. (4) can be written as

$$
\begin{aligned}
H = {} & \frac{1}{2\mu}\left[\left(1 - \frac{eB\theta}{4c\hbar}\right)p_x + \left(\frac{\eta}{2\hbar} - \frac{eB}{2c}\right)y\right]^2 \\
& + \frac{1}{2\mu}\left[\left(1 - \frac{eB\theta}{4c\hbar}\right)p_y - \left(\frac{\eta}{2\hbar} - \frac{eB}{2c}\right)x\right]^2 \\
& + \frac{1}{2}\mu\omega^2\left[\left(x - \frac{\theta}{2\hbar}p_y\right)^2 + \left(y + \frac{\theta}{2\hbar}p_x\right)^2\right]. \quad (8)
\end{aligned}
$$

The above expression can be more conveniently written in terms of the following frequencies:

$$\tilde{\omega} = \frac{eB}{2\mu c}, \qquad \omega_\theta = \frac{2\hbar}{\mu\theta}, \qquad \omega_\eta = \frac{\eta}{2\hbar\mu}. \qquad (9)$$

Then, we find

$$H_{\text{NC}} = \alpha\frac{p_x^2 + p_y^2}{2\mu} + \frac{1}{2}\mu\beta(x^2 + y^2) + \gamma(xp_y - yp_x), \quad (10)$$

where the constants α, β, γ are given by

$$\alpha = \left(1 - \frac{\tilde{\omega}}{\omega_\theta}\right)^2 + \frac{\omega^2}{\omega_\theta^2}, \qquad (11a)$$

$$\beta = (\tilde{\omega} - \omega_\eta)^2 + \omega^2, \qquad (11b)$$

$$\gamma = (\tilde{\omega} - \omega_\eta)\left(1 - \frac{\tilde{\omega}}{\omega_\theta}\right) - \frac{\omega^2}{\omega_\theta}. \qquad (11c)$$

Upon recognizing that the last term in Eq. (10) involves the z component of the canonical angular momentum operator $L_z^{\text{can}} = (\boldsymbol{r} \times \boldsymbol{p})_z = xp_y - yp_x$, the noncommutative Hamiltonian can be written in the following form:

$$H_{\text{NC}} = \sqrt{\alpha}\left\{\frac{p_x^2 + p_y^2}{2\frac{\mu}{\sqrt{\alpha}}} + \frac{1}{2}\frac{\mu}{\sqrt{\alpha}}\beta(x^2 + y^2) + \frac{\gamma}{\sqrt{\alpha}}L_z^{\text{can}}\right\}, \quad (12)$$

and therefore defining

$$M = \frac{\mu}{\sqrt{\alpha}}, \qquad (13a)$$

$$\Omega = \sqrt{\beta}, \qquad (13b)$$

we can finally write

$$H_{\text{NC}} = \sqrt{\alpha}\left[H_\circ^{\text{2D}} + \frac{\gamma}{\sqrt{\alpha}}L_z^{\text{can}}\right], \qquad (14)$$

where

$$H_\circ^{\text{2D}} = \frac{p_x^2 + p_y^2}{2M} + \frac{1}{2}M\Omega^2(x^2 + y^2). \qquad (15)$$

We see therefore that the Hamiltonian in Eq. (10) can be related to $H_\circ^{\text{2D}}$, the Hamiltonian of a well-known *and exactly solvable* nonrelativistic system, that of a two-dimensional isotropic (or circular) harmonic oscillator (of frequency Ω and mass M). The eigenfunctions and eigenvalues of this system are well known [38] and can be readily used to solve the noncommutative Hamiltonian of Eq. (14) since the angular momentum operator L_z^{can} commutes with $H_\circ^{\text{2D}}$. Thus, the complete set of eigenfunctions and the corresponding eigenvalues for the NC Hamiltonian are identified by a radial quantum number $n = 0, 1, 2, \ldots$ and the angular momentum quantum number $m = 0, \pm1, \pm2, \ldots$ [38] and are given by

$$\psi_{n,m}(r, \varphi) = C_{n,m}\, r^{|m|}\, e^{-\frac{r^2}{4a_B^2}}\, {}_1F_1\left(-n, |m| + 1; \frac{r^2}{2a_B^2}\right)e^{im\varphi}, \qquad (16a)$$

$$\varepsilon_{n,m} = \hbar\Omega(|m| + 1 + 2n)\sqrt{\alpha} + \hbar m\gamma, \qquad (16b)$$

where $a_B = \sqrt{\frac{\hbar}{2M\Omega}}$ and $C_{n,m}$ are normalization constants that can be easily computed as

$$C_{n,m} = \frac{a_B^{-(|m|+1)}}{\sqrt{\pi\, 2^{|m|+1}}}\frac{\sqrt{\Gamma(|m| + 1 + n)}}{\Gamma(|m| + 1)\sqrt{\Gamma(n + 1)}}. \qquad (17)$$

By setting $\omega = 0$ we obtain the results for the noncommutative charged particle in a magnetic field, which we will discuss as the commutative counterpart has already been studied [18]. At this point we digress a little to point out some features of the spectrum. We note that the spectrum is nondegenerate because of the presence of the last term on the right-hand side of Eq. (16b). However, one may easily verify that the usual degeneracy pattern is recovered when $\omega = 0$, $\theta = 0$. We shall see later that nondegeneracy of the spectrum has interesting consequences.

So far we have described the systems keeping both space as well as momentum noncommutativity. It may be noted that momentum noncommutativity ($\eta \neq 0$) produces a magnetic-field-like effect in the commutative plane while space noncommutativity ($\theta \neq 0$), although it affects other parameters like the mass, does not produce such a magnetic-field-like effect on the commutative plane. Thus, we shall henceforth consider only noncommuting momentum operators. Note that in this case the Hamiltonian can be written in the form

$$H = \frac{1}{2\mu}(\boldsymbol{p} - \boldsymbol{A})^2 + \frac{1}{2}\mu\omega^2(x^2 + y^2), \qquad (18)$$

where $\boldsymbol{A} = \frac{1}{2}[(-B + \frac{c\eta}{e\hbar})y, (B - \frac{c\eta}{e\hbar})x]$. In the case without the oscillator part, a critical value is found for the magnetic field B_{cr} for which the Hamiltonian becomes that of a free particle of mass M given by (13). Imposing the condition $\Omega = 0$ one immediately gets the value of the critical field:

$$B_{\text{cr}} = \frac{\eta c}{\hbar e}. \qquad (19)$$

On the other end it is easily seen that when the oscillator is present ($\omega \neq 0$), then the equation $\Omega = 0$ does not have (real) solutions, implying that in this case there is no critical value of the magnetic field.

III. ANGULAR MOMENTUM BACKFLOW ON THE NONCOMMUTATIVE PLANE

Before studying angular momentum backflow, let us note that the current density for a state described by the wave function Ψ is given by

$$\boldsymbol{j} = \frac{\hbar}{2Mi}(\Psi^*\nabla\Psi - \Psi\nabla\Psi^*) - \frac{e}{Mc}\boldsymbol{A}\Psi^*\Psi.$$
$$= \boldsymbol{j}_1 - \boldsymbol{j}_2. \qquad (20)$$

It may be noted that in terms of cylindrical polar coordinates, the vector potential can be written as

$$A_r = 0, \quad A_\varphi = \frac{1}{2}\left(B - \frac{c\eta}{e\hbar}\right)r. \qquad (21)$$

Next, we discuss a very important concept, namely, that of effective angular momentum. The effective angular momentum $\ell_{\text{eff}} = \hbar m_{\text{eff}}$ is defined through [18]

$$m_{\text{eff}}(r, \varphi) = \frac{\partial}{\partial \varphi} \text{Arg } \Psi(r, \varphi) = \text{Im} \frac{\partial \Psi(r, \varphi)/\partial \varphi}{\Psi(r, \varphi)} \quad (22a)$$

$$= \left(\frac{\mu \, r}{\hbar}\right) \frac{\boldsymbol{e}_\varphi \cdot \boldsymbol{j}_1(r, \varphi)}{\rho}, \quad (22b)$$

where $\Psi(r, \varphi)$ denotes the wave function in the amplitude-phase form

$$\Psi(r, \varphi) = \sqrt{\rho(r, \varphi)} \exp\left[i \int_0^\varphi d\varphi' m_{\text{eff}}(r, \varphi')\right], \quad (23)$$

$\boldsymbol{e}_\varphi \cdot \boldsymbol{j}_1(r, \varphi)$ being the probability current along the azimuthal direction and $\rho = |\Psi(r, \varphi)|^2$ is the probability density [38].

A. Model without oscillator interaction: $\omega = 0$

Now we consider a specific example of a (normalized) wave function which is a simple sum of three eigenfunctions, as given by Eq. (16). We consider only the $n = 0$ states with three different, nonpositive, magnetic quantum numbers $(-2, -1, 0)$. For the sake of comparison, this is analogous to what has been done in [18] and allows to compute explicitly the local effective magnetic quantum number $m_{\text{eff}}(r, \varphi)$ in

a simple closed form. Using Eq. (16) we obtain the state $\Psi_0(r, \varphi)$ as

$$\Psi_0(r, \varphi) = \frac{1}{\sqrt{3}} \sum_{m=0}^{2} c_m(r) e^{-im\varphi}$$

$$= \frac{1}{\sqrt{3}}[c_0(r) + c_1(r)e^{-i\varphi} + c_2(r)e^{-2i\varphi}], \quad (24)$$

where the coefficients $c_m(r)$ are given by

$$c_m(r) = C_{0,m} r^{|m|} e^{-\frac{r^2}{4a_B^2}}, \quad (25)$$

and we note that $C_{0,m} = C_{0,-m} = C_{0,|m|}$ as given by Eq. (17). Note that the state in Eq. (24) is a simple sum of three eigenstates from Eq. (16a) with $n = 0$ and angular momentum $L_z^{\text{can}} = -\hbar(0, 1, 2)$, respectively.

It is important to note that, in the model without oscillator interaction, an infinite degeneracy for fixed n and nonpositive m is present, therefore, for our wave function, time dependence occurs only in the form of an immaterial global phase. Time dependence for the model with oscillator interaction will be discussed in Sec. III B.

From Eq. (22a) we can determine the effective value of the quantum number $m_{\text{eff}}(r, \varphi)$ for the superposition in Eq. (24):

$$m_{\text{eff}}(r, \varphi) = -\frac{c_1^2 + 2c_2^2 + c_0 c_1 \cos\varphi + 3c_1 c_2 \cos\varphi + 2c_0 c_2 \cos 2\varphi}{c_0^2 + c_1^2 + c_2^2 + 2c_0 c_1 \cos\varphi + 2c_1 c_2 \cos\varphi + 2c_0 c_2 \cos 2\varphi}. \quad (26)$$

In order to have $m_{\text{eff}} > 0$, we need to look for values of (r, φ) where m_{eff} passes through zero. This leads to

$$\sqrt{2}r \cos^2\varphi + \left(\frac{a_B}{\sqrt{2}} + \frac{3r^2}{4a_B}\right) \cos\varphi + \frac{r^3}{4a_B^2} + \left(\frac{1 - \sqrt{2}}{2}\right)r = 0. \quad (27)$$

In the noncommutative setting the form of Eq. (27) remains the same for both models and the differences lie in the different dependence of frequency and mass contained in a_B on the parameter η. To make an easy comparison with different models, it is convenient to describe the system in dimensionless units by using the parameter a_B as a unit of length, thus, in general, we will use the value a_B as in the commutative setting. It is important to note that, as the magnetic field changes, a_B also changes, which means that the unit of length will change as well. We recall that in some previous works a bound on the parameter η was obtained by comparing noncommutative predictions with measurements and is given by [31,36]

$$\sqrt{\eta} \lesssim 2.26 \frac{\mu\text{eV}}{c}. \quad (28)$$

Thus, we set $\eta/m_e^2 c^2 = 10^{-25}$, m_e being the electron mass and it is consistent with (28). Next, choosing different values of the magnetic field around the critical value B_{cr}, given in Eq. (19), we determine the regions of quantum backflow and the results are given in Fig. 1.

As expected from Eq. (27), the backflow area changes only radially. To understand how the parameters contribute to the value of a_B we have to study Eq. (13) with $\omega = 0$. Approach-

ing the value B_{cr}, backflow extends radially to infinity since Ω tends to zero and thus a_B tends to infinity, in the limit of small magnetic field the dominant contribution to Ω is due to the parameter η which is constant, in the limit of large magnetic field we return to the commutative case. This is evident if we look at Fig. 2 where the backflow area has been plotted as a function of the magnetic field. The unit of area has been chosen as a fixed value of $a_{B_{cr}}^2$ where $\eta = 10^{-25} m_e^2 c^2$ to be able to make a comparison between areas at different values of the magnetic field. The magnetic field is expressed in units B_{cr} where $\eta = 10^{-25} m_e^2 c^2$.

Next, we consider a (normalized) superposition of eigenfunctions consisting of a larger number N, instead of just 3 as in Eq. (24), of angular momentum eigenstates of the form

$$\Psi_0(r, \varphi) = \frac{1}{\sqrt{N}} \sum_{m=0}^{N-1} c_m(r) e^{-im\varphi} \quad (29)$$

that is a linear combination of N components with nonpositive angular momentum ($L_z^{\text{can}} = -\hbar m \leqslant 0$). The coefficients $c_m(r)$ are defined as in Eq. (25). In the $\omega = 0$ setting we get the results shown in Fig. 3 by repeating the same steps we already showed for the case of three eigenfunctions. We note that the behavior of this system is exactly the same as in the
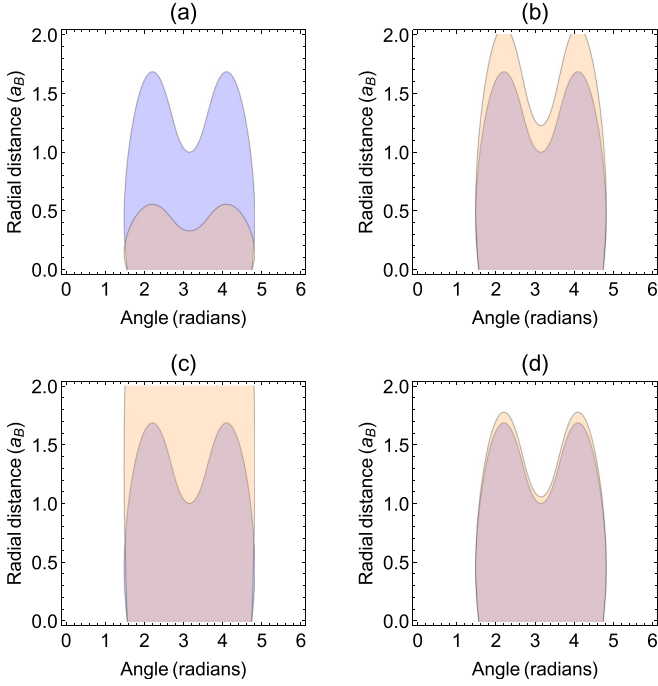
FIG. 1. Plot of the region (shaded area) where $m_{\text{eff}} > 0$ in the (r, φ) plane for the commutative case (blue) and the noncommutative case with $\eta/m_e^2 c^2 = 10^{-25}$ (orange) with $\omega = 0$. The values of the magnetic field are $B/B_{\text{cr}} = 0.1$ (a), $B/B_{\text{cr}} = 0.6$ (b), $B/B_{\text{cr}} = 0.9$ (c), $B/B_{\text{cr}} = 10$ (d). The radial distance r is in units of a_B.

FIG. 3. Plot of the region (shaded area) where $m_{\text{eff}} > 0$ in the (r, φ) plane for the commutative case (blue) and the noncommutative case with $\eta/m_e^2 c^2 = 10^{-25}$ (orange) with $\omega = 0$ for a state with $N = 11$ components as in Eq. (29). The values of the magnetic field are (a) $B/B_{\text{cr}} = 0.1$, (b) $B/B_{\text{cr}} = 0.6$, (c) $B/B_{\text{cr}} = 0.9$, (d) $B/B_{\text{cr}} = 10$. The radial distance r is in units of a_B.

previous case, and thus we come to the conclusion that, for $n = 0$, the equation that gives us the points (r, φ) for which m_{eff} passes through zero, can always be written in the form $f(r/a_B, \varphi) = 0$, where f will be given by a function similar to that given in Eq. (27) but with a larger number of terms since we are here considering a state Ψ with $N = 11$ components, as in Eq. (29). Therefore, compared to the results in [18] (solid line in Fig. 3), the shape of the region with backflow is similar to the noncommutative case (dashed line) but with the radial
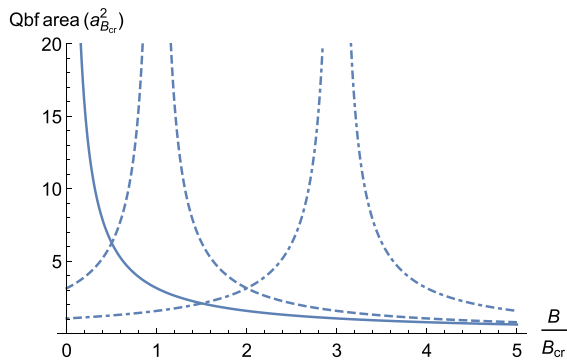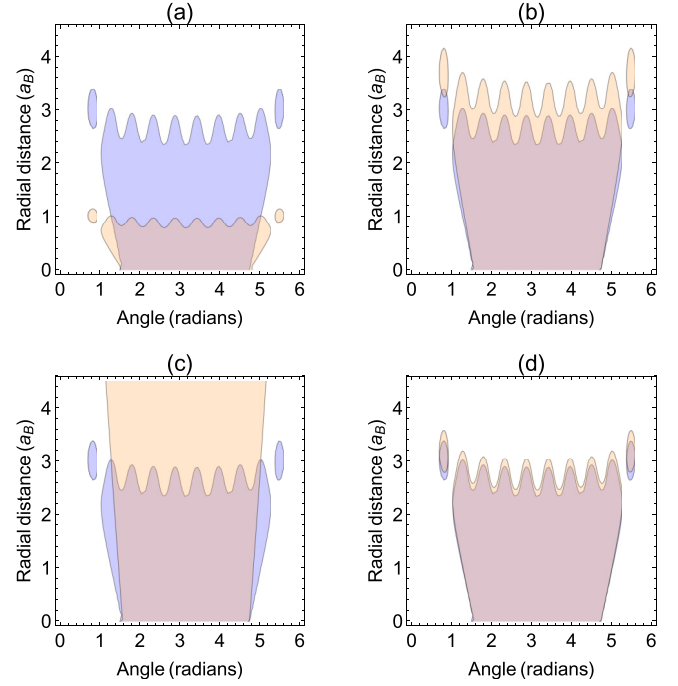

FIG. 2. Plot of the backflow area (in units of $a_{B_{cr}}^2$) as a function of the magnetic field for a state with three components as in Eq. (24) and for two values of the parameter η with $\omega = 0$, $\eta_1 = 10^{-25} m_e^2 c^2$ (dashed line), $\eta_2 = 3 \times 10^{-25} m_e^2 c^2$ (dotted-dashed line) compared to the commutative result (solid line).

extension being mostly affected when changing the value of the magnetic field.

B. Model with oscillator interaction: $\omega \neq 0$

In this section we shall analyze the effect of the oscillator interaction on the angular momentum backflow. It may be noted that when an oscillator interaction is present, a critical field can not be defined as before: at least in the sense that there is no value of B that makes the Hamiltonian H in Eq. (12) that of a free particle. The value B_{cr} in this case simply minimizes the quantity β in Eq. (11c) and thus Ω. We can therefore say that the field B_{cr} minimizes in this instance the interaction.

Nonetheless, for the sake of convenience we shall make our plots with respect to B/B_{cr}. First of all we note that the infinite degeneracy for fixed n and nonpositive values of m is no longer present when considering the oscillator interaction. Indeed, from Eq. (16b) we see that, when $\theta = 0$, $\omega_\theta \to \infty$, $\alpha \to 1$, $\Omega = \sqrt{\beta} \to \gamma$ and so when $m \geqslant 0$ there is degeneracy with respect to m. Clearly, such degeneracy is lifted when the oscillator frequency $\omega \neq 0$ because in this case $\Omega = \sqrt{\beta} \neq \gamma$. This in turn introduces a time dependence in the wave function of Eq. (24) because each component will have now a different energy eigenvalue. This in turn leads to a time dependence of the effective magnetic quantum

number m_{eff} and leads to

$$m_{\text{eff}}(r, \varphi, t) = -\frac{c_1^2 + 2c_2^2 + c_0 c_1 \cos\left[\varphi + (\epsilon_{-1} - \epsilon_0)\frac{t}{\hbar}\right] + 3c_1 c_2 \cos\left[\varphi + (\epsilon_{-2} - \epsilon_{-1})\frac{t}{\hbar}\right] + 2c_0 c_2 \cos\left[2\varphi + (\epsilon_{-2} - \epsilon_0)\frac{t}{\hbar}\right]}{c_0^2 + c_1^2 + c_2^2 + 2c_0 c_1 \cos\left[\varphi + (\epsilon_{-1} - \epsilon_0)\frac{t}{\hbar}\right] + 2c_1 c_2 \cos\left[\varphi + (\epsilon_{-2} - \epsilon_{-1})\frac{t}{\hbar}\right] + 2c_0 c_2 \cos\left[2\varphi + (\epsilon_{-2} - \epsilon_0)\frac{t}{\hbar}\right]},$$
(30)

where $\epsilon_m = \epsilon_{0,m}$. The time dependence reduces to a translation of the angle in m_{eff}. This effect is shown explicitly in Fig. 4, where we plot the backflow region in the (r, φ) plane for two different time values (see caption of figure). We show the region for $t = 0$ (delimited by the dashed curve) which corresponds exactly to the time-independent case of Eq. (26) while the solid curve delimits the φ shifted one corresponding to Eq. (30). The area of the quantum backflow area will be the same.

Next, we show in Fig. 5 the area of the quantum backflow regions as function of the external magnetic field expressed in units of the critical magnetic field B_{cr} given by Eq. (19). In Fig. 5 the solid line is the value of the area of the quantum backflow region when the oscillator interaction is absent. At $B = B_{\text{cr}}$ the system becomes free and the region where there is backflow is infinite. On the contrary, when the oscillator interaction is present the quantity β in Eq. (11b) does not vanish and thus the system is always bounded and the backflow region is always finite. The larger the oscillator frequency ω, the stronger this effect (smaller area) as we can see by comparing in Fig. 5 the dashed line ($\omega = 0.3\,\omega_\eta$) and the dotted-dashed line ($\omega = \omega_\eta$).

IV. BACKFLOW PROBABILITY

In the previous sections we have essentially visualized the amount of quantum backflow by showing the area in the (r, φ) plane where the effective angular momentum becomes positive having considered a quantum state built out of components with only nonpositive values of m. We have also compared various scenarios by computing numerically the backflow area. Nevertheless, it would be clearly interesting to have a quantitative estimate of the quantum backflow. One of the ways to obtain this estimate is to introduce the concept of probability associated with angular momentum backflow. While in the case of one-dimensional problems the issue of the backflow probability has been discussed at length [5,12,39,40], it has not been studied within the context of a two-dimensional interacting system. Perhaps this was due to the difficulties stemming from the two-dimensional nature of the problem.

A particularly useful approach for the computation of the total backflow probability has been proposed in [12]. In this approach, for a quantum state built with only positive momenta the total backflow probability is related, for a one-dimensional problem, to the fraction of the x axis where the local wave number $k(x)$ becomes negative. Here we extend this concept to the case of an interacting two-dimensional problem. Our state $\Psi(r, \varphi)$ defined in Eq. (24) is a linear combination of eigenfunctions (16a) with nonpositive values of the angular momentum (L_z^{can} component) or nonpositive values of the magnetic quantum number m ($m \leqslant 0$). In our problem the analog of the local wave number $k(x)$ of [12] is the local angular momentum (L_z^{can} component) $\ell(\mathbf{r}) = \hbar m_{\text{eff}}(\mathbf{r})$. For a system for which the positions $\mathbf{r}$ are distributed according to a normalizable probability distribution $|\Psi(\mathbf{r})|^2$, the probability distribution of the angular momentum is

$$P(\ell) = \iint |\Psi(\mathbf{r})|^2 \, \delta(\ell(\mathbf{r}) - \ell) \, d^2\mathbf{r}. \tag{31}$$

The above relation can be understood noting that $P(\ell)d\ell$ is the probability of having an angular momentum between ℓ and $\ell + d\ell$, and this can be estimated by averaging over the
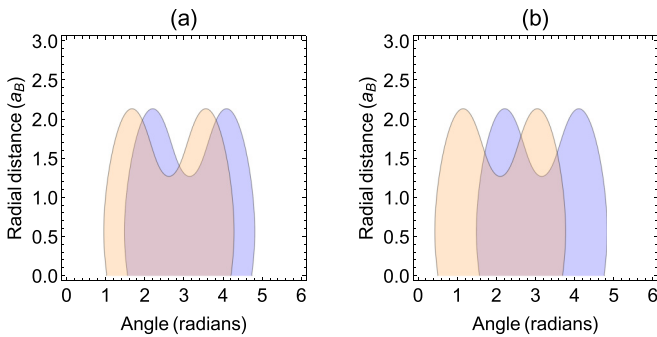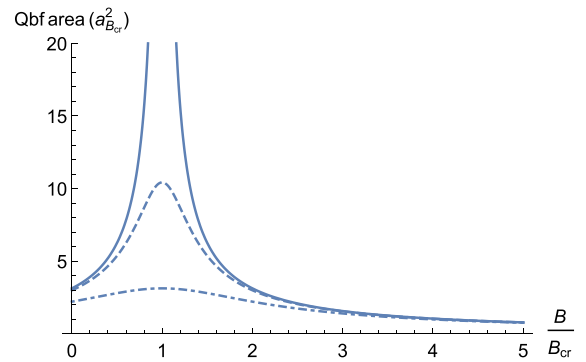

FIG. 4. Plot of the region (shaded area) where $m_{\text{eff}} > 0$ for two values of time (orange), compared to the result at $t = 0$ (blue), in the (r, φ) plane. The values of time are $t_a = \frac{t_{2\pi}}{12}$ and $t_b = \frac{t_{2\pi}}{6}$, where $t_{2\pi} = 2\pi\frac{\hbar}{\epsilon_{-1}-\epsilon_0}$ is the time relative to a 2π shift, which depends on the magnetic field. Here we consider the case with the oscillator ($\omega = 0.8\,\omega_\eta$ with $\eta/m_e^2 c^2 = 10^{-25}$) for a single value of the magnetic field. The radial distance r is in units of a_B.

FIG. 5. Plot of the backflow area (in units of $a_{B_{cr}}^2$), for a state with three components as in Eq. (24) or as in Eq. (29) with $N = 3$, as a function of the magnetic field (in B_{cr} units where $\eta = 10^{-25}m_e^2 c^2$), for two values of the oscillator frequency [$\omega_1 = 0.3\,\omega_\eta$ (dashed line), $\omega_2 = \omega_\eta$ (dotted-dashed line)] compared to the result without oscillator (solid line).

positions r for which $\ell(r) = \ell$ which are distributed according to $|\Psi(r)|^2$.

It is convenient, in the following, to define a probability density with respect to the angular momentum (magnetic) quantum number $m = \ell/\hbar$. This is easily done by extracting the constant $\hbar$ from the δ function and defining $P(m) = \hbar P(\ell)$:

$$P(m) = \iint |\Psi(r)|^2 \, \delta(m_{\text{eff}}(r) - m) \, d^2r, \quad (32)$$

so that the total backflow probability (probability of having a positive m) is obtained as

$$P_{\text{backflow}} = \int_0^\infty P(m) \, dm. \quad (33)$$

Inserting Eq. (32) into Eq. (33) and making use of the fact that the Dirac δ function is the derivative of the Heaviside θ function we obtain

$$P_{\text{backflow}} = \iint |\Psi(r)|^2 \, d^2r \int_0^{+\infty} \left\{ -\frac{\partial}{\partial m} \theta(m_{\text{eff}}(r) - m) \right\} dm$$

$$= \iint |\Psi(r)|^2 \, d^2r \left[-\theta(m_{\text{eff}}(r) - m) \right]_{m=0}^{m=+\infty}$$

$$= \iint |\Psi(r)|^2 \, \theta(m_{\text{eff}}(r)) \, d^2r. \quad (34)$$

We may finally write the total angular momentum backflow probability as

$$P_{\text{backflow}} = \int_0^\infty \int_0^{2\pi} \theta(m_{\text{eff}}(r, \varphi)) \, |\Psi(r, \varphi)|^2 \, r \, dr \, d\varphi, \quad (35)$$

where $\Psi(r, \varphi)$ is the normalized eigenfunction.

We have computed the total angular momentum backflow probability P_{backflow} evaluating numerically the integral in Eq. (35) first for an effective angular momentum defined in Eq. (26) for the state as in Eq. (24) with a number of components $N = 3$, and subsequently for states defined as in Eq. (29) with increasing number of components up to $N = 6$.

We have also examined the variation of the probability of quantum backflow with respect to different choices of the associated weights c_m with a given number of components N. The results of the computations are given in Table I where we see that P_{backflow} varies somewhat as the number of components of the state N is increased and, within a fixed N, as configurations with different weights c_m are considered. In some cases ($N = 3, 5, 6$) it appears that the configurations with c_0 the largest weight have a higher probability relative to the configurations where weights other than c_0 are largest but we were unable to generalize it. For instance, this does not happen for $N = 4$. This may be traced to the fact that the region where $m_{\text{eff}} > 0$ is strongly dependent on the different choices of the weights and also on the different values of N as we have explicitly observed. Also, as N increases, the computation becomes increasingly challenging from the numerical point of view. We have verified that, as expected, for any state with given number of components N and any configurations of the coefficients c_m, the backflow probability is independent of the magnetic field B computing P_{backflow} for two different values of the magnetic field. In retrospect, the independence of the total angular momentum backflow probability from the external magnetic field can be understood also from Eqs. (20)

TABLE I. Total backflow probability (P_{backflow}) computed numerically via Eq. (35) with an accuracy of one part in 10^3 for $N = 3, 4, 5, 6$ and different choices of the coefficients c_m for any given number of components N. The states considered here are all with the lowest value of the radial quantum number ($n = 0$) and no oscillator interaction ($\omega = 0$).

N	$(c_0, c_1, \ldots, c_{N-1})$	P_{backflow}
3	$\left(\frac{1}{\sqrt{3}}, \frac{1}{\sqrt{3}}, \frac{1}{\sqrt{3}}\right)$	0.049
	$\left(\frac{1}{\sqrt{2}}, \frac{1}{\sqrt{4}}, \frac{1}{\sqrt{4}}\right)$	0.103
	$\left(\frac{1}{\sqrt{4}}, \frac{1}{\sqrt{2}}, \frac{1}{\sqrt{4}}\right)$	0.023
	$\left(\frac{1}{\sqrt{4}}, \frac{1}{\sqrt{4}}, \frac{1}{\sqrt{2}}\right)$	0.032
4	$\left(\frac{1}{\sqrt{4}}, \frac{1}{\sqrt{4}}, \frac{1}{\sqrt{4}}, \frac{1}{\sqrt{4}}\right)$	0.052
	$\left(\frac{1}{\sqrt{2}}, \frac{1}{\sqrt{6}}, \frac{1}{\sqrt{6}}, \frac{1}{\sqrt{6}}\right)$	0.049
	$\left(\frac{1}{\sqrt{6}}, \frac{1}{\sqrt{2}}, \frac{1}{\sqrt{6}}, \frac{1}{\sqrt{6}}\right)$	0.016
	$\left(\frac{1}{\sqrt{6}}, \frac{1}{\sqrt{6}}, \frac{1}{\sqrt{2}}, \frac{1}{\sqrt{6}}\right)$	0.038
	$\left(\frac{1}{\sqrt{6}}, \frac{1}{\sqrt{6}}, \frac{1}{\sqrt{6}}, \frac{1}{\sqrt{2}}\right)$	0.031
5	$\left(\frac{1}{\sqrt{5}}, \frac{1}{\sqrt{5}}, \frac{1}{\sqrt{5}}, \frac{1}{\sqrt{5}}, \frac{1}{\sqrt{5}}\right)$	0.051
	$\left(\frac{1}{\sqrt{2}}, \frac{1}{\sqrt{8}}, \frac{1}{\sqrt{8}}, \frac{1}{\sqrt{8}}, \frac{1}{\sqrt{8}}\right)$	0.192
	$\left(\frac{1}{\sqrt{8}}, \frac{1}{\sqrt{2}}, \frac{1}{\sqrt{8}}, \frac{1}{\sqrt{8}}, \frac{1}{\sqrt{8}}\right)$	0.011
	$\left(\frac{1}{\sqrt{8}}, \frac{1}{\sqrt{8}}, \frac{1}{\sqrt{2}}, \frac{1}{\sqrt{8}}, \frac{1}{\sqrt{8}}\right)$	0.016
	$\left(\frac{1}{\sqrt{8}}, \frac{1}{\sqrt{8}}, \frac{1}{\sqrt{8}}, \frac{1}{\sqrt{2}}, \frac{1}{\sqrt{8}}\right)$	0.025
	$\left(\frac{1}{\sqrt{8}}, \frac{1}{\sqrt{8}}, \frac{1}{\sqrt{8}}, \frac{1}{\sqrt{8}}, \frac{1}{\sqrt{2}}\right)$	0.029
6	$\left(\frac{1}{\sqrt{6}}, \frac{1}{\sqrt{6}}, \frac{1}{\sqrt{6}}, \frac{1}{\sqrt{6}}, \frac{1}{\sqrt{6}}, \frac{1}{\sqrt{6}}\right)$	0.047
	$\left(\frac{1}{\sqrt{2}}, \frac{1}{\sqrt{10}}, \frac{1}{\sqrt{10}}, \frac{1}{\sqrt{10}}, \frac{1}{\sqrt{10}}, \frac{1}{\sqrt{10}}\right)$	0.218
	$\left(\frac{1}{\sqrt{10}}, \frac{1}{\sqrt{2}}, \frac{1}{\sqrt{10}}, \frac{1}{\sqrt{10}}, \frac{1}{\sqrt{10}}, \frac{1}{\sqrt{10}}\right)$	0.014
	$\left(\frac{1}{\sqrt{10}}, \frac{1}{\sqrt{10}}, \frac{1}{\sqrt{2}}, \frac{1}{\sqrt{10}}, \frac{1}{\sqrt{10}}, \frac{1}{\sqrt{10}}\right)$	0.011
	$\left(\frac{1}{\sqrt{10}}, \frac{1}{\sqrt{10}}, \frac{1}{\sqrt{10}}, \frac{1}{\sqrt{2}}, \frac{1}{\sqrt{10}}, \frac{1}{\sqrt{10}}\right)$	0.020
	$\left(\frac{1}{\sqrt{10}}, \frac{1}{\sqrt{10}}, \frac{1}{\sqrt{10}}, \frac{1}{\sqrt{10}}, \frac{1}{\sqrt{2}}, \frac{1}{\sqrt{10}}\right)$	0.023
	$\left(\frac{1}{\sqrt{10}}, \frac{1}{\sqrt{10}}, \frac{1}{\sqrt{10}}, \frac{1}{\sqrt{10}}, \frac{1}{\sqrt{10}}, \frac{1}{\sqrt{2}}\right)$	0.023

and (22). Indeed, we see that the term j_2 in the total current, which depends explicitly on the magnetic field (vector potential), does not contribute to m_{eff}. On the other hand, from the explicit expression of the exact wave functions [cf. Eq. (16)] the only other dependence on the magnetic field is through the quantity a_B. Given that the wave functions depend only on $(r/a_B, \varphi)$ and that $|\Psi(r)|^2 \propto a_B^{-2} f(r/a_B, \varphi)$, it can be easily shown from Eq. (35) that the total backflow probability is independent of the magnetic field B. Let us also remark that while the results in Table I have been computed for $\omega = 0$, choosing an oscillator interaction $\omega \neq 0$ simply changes the value of a_B but not P_{backflow} since we have shown that the probability is a_B independent.

V. DISCUSSION AND CONCLUSIONS

In this article we have studied the noncommutative generalization of the angular momentum backflow problem considered in [18]. Extending the exact solution of a free-charged particle in a homogeneous magnetic field, we have also

considered angular momentum backflow when an oscillator interaction is present. Subsequently, we also included momentum noncommutativity only so as to avoid gauge invariance issues associated with noncommuting space coordinates [31]. It has been found that the area where angular momentum backflow takes place changes with the magnetic field, which in turn depends on the noncommutativity parameter.

Next, we have attempted to give a quantitative description of the angular momentum backflow. We adopted the approach developed in [12] where in a one-dimensional problem the total probability of momentum backflow is related to the fraction of the x axis where the local wave number $k(x)$ is negative (within a state consisting only of components with positive wave numbers). We therefore extend the above approach [12] to our two-dimensional problem of a charged Dirac particle in a magnetic field. More precisely, in analogy with [18] we considered a (normalized) physical state $\Psi(\mathbf{r})$ consisting of a linear combination of eigenfunctions with nonpositive magnetic angular momentum values ($m \leqslant 0$) [cf. Eq. (24)] and relate the probability of backflow to an average, over the probability density distribution $|\Psi(\mathbf{r})|^2$, of the area of the region of the plane where $m_{\text{eff}} \geqslant 0$ [cf. Eqs. (33) and (35)]. It has been found that total probability of angular momentum backflow remains the same for different values of the magnetic field. In other words, the backflow probability is independent of the magnetic field.

It might be noticed that our study of the backflow regions is based on the analysis of the quantity m_{eff} defined in Eqs. (22a) and (22b) and as such it is not a gauge-invariant quantity because only the total current $\mathbf{j}$ of Eq. (19) is gauge invariant while $\mathbf{j}_1$ and $\mathbf{j}_2$ are gauge variant. So, quantities obtained as averages over the effective local angular momentum $m_{\text{eff}}(r, \varphi)$ such as the expectation value of the canonical angular momentum $\langle \psi | L_z^{\text{can}} | \psi \rangle = \int d^2\mathbf{r}\, m_{\text{eff}}(r, \varphi) \, |\psi|^2$ would be gauge variant. This might worry the reader that our conclusions on the angular momentum backflow depend on the gauge choice. However, this is not the case as there is a well-known subtlety concerning the gauge-invariant definition of the orbital angular momentum in the Landau problem [41–44]. Indeed, it has been shown that a gauge-invariant orbital angular momentum L_z can be defined in terms of the canonical angular momentum $L_z^{\text{can}} = (\mathbf{r} \times \mathbf{p})_z$ via $L_z = L_z^{\text{can}} + \frac{e}{c} r A_\varphi - \frac{e}{2c} B r^2$ [43]. However, it turns out that in the symmetric gauge, used throughout this work, the additional contribution $\frac{e}{c} r A_\varphi - \frac{e}{2c} B r^2$ vanishes identically and the expectation values of L_z^{can}, computed with m_{eff}, coincide with the expectation values of the gauge invariant L_z. Going to another gauge, for instance the Landau gauge, the change in $\langle L_z^{\text{can}} \rangle$ will be compensated by the change in $\langle (\frac{e}{c} r A_\varphi - \frac{e}{2c} B r^2) \rangle$ as to obtain the same result of the sym-

metric gauge. By the same token, other observable quantities computed, in the symmetric gauge from m_{eff} such as, for instance, the backflow probability, are gauge invariant.

We have also examined the dependence of the quantum backflow probability with respect to the number of components (N) in the wave packet as well as the associated weights c_m finding that it can reach values as high as $P_{\text{backflow}} \approx 0.2$. More precisely, in this paper we have considered states of the system which are either (i) only a simple sum of the N eigenstates with a fixed value of the radial quantum number ($n = 0$) or (ii) a sum of N components (again with $n = 0$) with various choices of different weights c_m. We have not been able to identify a well-defined and general pattern of P_{backflow} when higher values of the number of components N are considered, both in configurations with equal and different weights c_m. Other possibilities could of course be considered, but they would go beyond the scope of this work. Here, we were mainly interested in presenting a sensible definition of the angular momentum backflow probability for the problem of a charged particle in a constant homogeneous magnetic field, with and without the oscillator interaction, along with a complete and exact solution, of the same problem, also in the presence of noncommutative coordinates. One interesting feature that emerges from our analysis is that the angular momenutm backflow probability in our two-dimensional system reaches, in some cases, values ($P_{\text{backflow}} \approx 0.2$) that are larger than the maximum allowed value found by Braken and Malloy $c_{bm} \approx 0.04$ for a one-dimensional free system. This may be quite important in view of upcoming experimental studies of the quantum backflow.

In conclusion, in this paper we have been able to confirm the angular momentum backflow of a nonrelativistic charged particle in a magnetic field even in the presence of noncommutative coordinates. We also succeeded in defining and computing explicitly the angular momentum total backflow probability P_{backflow}, going beyond the results of Ref. [18] by extending to a two-dimensional physical system the approach developed in [12] for momentum backflow in a one-dimensional system.

It is the authors' opinion that these findings are of interest for further developments in the subject of quantum backflow.

ACKNOWLEDGMENTS

[1] G. R. Allcock, The time of arrival in quantum mechanics I. Formal considerations, Ann. Phys. **53**, 253 (1969).

[2] G. R. Allcock, The time of arrival in quantum mechanics II. The individual measurement, Ann. Phys. **53**, 286 (1969).

[3] G. R. Allcock, The time of arrival in quantum mechanics III. The measurement ensemble, Ann. Phys. **53**, 311 (1969).

[4] A. J. Bracken and G. F. Melloy, Probability backflow and a new dimensionless quantum number, J. Phys. A: Math. Gen. **27**, 2197 (1994).

[5] J. M. Yearsley, J. J. Halliwell, R. Hartshorn, and A. Whitby, Analytical examples, measurement models, and classical limit of quantum backflow, Phys. Rev. A **86**, 042116 (2012).

[6] G. F. Melloy and A. J. Bracken, Probability backflow for a Dirac particle, Found. Phys. **28**, 505 (1998).

[7] G. F. Melloy and A. J. Bracken, The velocity of probability transport in quantum mechanics, Ann. Phys. **7**, 726 (1998).

[8] H.-Y. Su and J.-L. Chen, Quantum backflow in solutions to the Dirac equation of the spin-1/2 free particle, Mod. Phys. Lett. A **33**, 1850186 (2018).

[9] J. Ashfaque, J. Lynch, and P. Strange, Relativistic quantum backflow, Phys. Scr. **94**, 125107 (2019).

[10] C. J. Fewster, S. P. Eveson, and R. Verch, Quantum inequalities in quantum mechanics, Ann. Henri Poincaré **6**, 1 (2005).

[11] M. Penz, G. Grübl, S. Kreidl, and P. Wagner, A new approach to quantum backflow, J. Phys. A: Math. Gen. **39**, 423 (2005).

[12] M. V. Berry, Quantum backflow, negative kinetic energy, and optical retro-propagation, J. Phys. A: Math. Theor. **43**, 415302 (2010).

[13] W. van Dijk and F. M. Toyama, Decay of a quasistable quantum system and quantum backflow, Phys. Rev. A **100**, 052101 (2019).

[14] M. Barbier, Quantum backflow for many-particle systems, Phys. Rev. A **102**, 023334 (2020).

[15] A. Goussev, Equivalence between quantum backflow and classically forbidden probability flow in a diffraction-in-time problem, Phys. Rev. A **99**, 043626 (2019).

[16] A. Goussev, Probability backflow for correlated quantum states, Phys. Rev. Res. **2**, 033206 (2020).

[17] H. Bostelmann, D. Cadamuro, and G. Lechner, Quantum backflow and scattering, Phys. Rev. A **96**, 012112 (2017).

[18] P. Strange, Large quantum probability backflow and the azimuthal angle–angular momentum uncertainty relation for an electron in a constant magnetic field, Eur. J. Phys. **33**, 1147 (2012).

[19] A. Goussev, Quantum backflow in a ring, arXiv:2008.08022.

[20] M. R. Douglas and N. A. Nekrasov, Noncommutative field theory, Rev. Mod. Phys. **73**, 977 (2001).

[21] M. R. Douglas, A. Connes, and A. Schwarz, Noncommutative geometry and matrix theory, J. High Energy Phys. 02 (1998) 003.

[22] N. Seiberg and E. Witten, String theory and noncommutative geometry, J. High Energy Phys. 09 (1999) 032.

[23] V. P. Nair and A. P. Polychronakos, Quantum mechanics on the noncommutative plane and sphere, Phys. Lett. B **505**, 267 (2001).

[24] S. Bellucci, A. Nersessian, and C. Sochichiu, Two phases of the noncommutative quantum mechanics, Phys. Lett. B **522**, 345 (2001).

[25] A. Smailagic and E. Spallucci, Noncommutative 3d harmonic oscillator, J. Phys. A: Math. Gen. **35**, L363 (2002).

[26] M. Loewe, J. Gamboa, F. Méndez, and J. C. Rojas, Noncommutative quantum mechanics: The two-dimensional central field, Int. J. Mod. Phys. A **17**, 2555 (2002).

[27] M. L. J. Gamboa, F. Mendez, and J. C. Rojas, The Landau problem and noncommutative quantum mechanics, Mod. Phys. Lett. A **16**, 2075 (2001).

[28] M. Chaichian, M. M. Sheikh-Jabbari, and A. Tureanu, Hydrogen Atom Spectrum and the Lamb Shift in Noncommutative QED, Phys. Rev. Lett. **86**, 2716 (2001).

[29] M. Chaichian, M. M. Sheikh-Jabbari, and A. Tureanu, Noncommutativity of space-time and the hydrogen atom spectrum, Eur. Phys. J. C **36**, 251 (2004).

[30] O. Panella and P. Roy, Quantum phase transitions in the noncommutative Dirac oscillator, Phys. Rev. A **90**, 042111 (2014).

[31] O. Bertolami and R. Queiroz, Phase-space noncommutativity and the Dirac equation, Phys. Lett. A **375**, 4116 (2011).

[32] C. Duval and P. A. Horváthy, Exotic galilean symmetry in the non-commutative plane and the Hall effect, J. Phys. A: Math. Gen. **34**, 10097 (2001).

[33] Ö. F. Dayi and A. Jellal, Hall effect in noncommutative coordinates, J. Math. Phys. **43**, 4592 (2002).

[34] M. Palmero, E. Torrontegui, J. G. Muga, and M. Modugno, Detecting quantum backflow by the density of a Bose-Einstein condensate, Phys. Rev. A **87**, 053618 (2013).

[35] Y. Eliezer, T. Zacharias, and A. Bahabad, Observation of optical backflow, Optica **7**, 72 (2020).

[36] O. Bertolami, J. G. Rosa, C. M. L. de Aragão, P. Castorina, and D. Zappalà, Noncommutative gravitational quantum well, Phys. Rev. D **72**, 025010 (2005).

[37] A. Kokado, T. Okamura, and T. Saito, Noncommutative quantum mechanics and the Seiberg-Witten map, Phys. Rev. D **69**, 125007 (2004).

[38] S. Flügge, *Practical Quantum Mechanics. I, II* (Springer, Berlin, 1974).

[39] J. M. Yearsley, Quantum arrival time for open systems, Phys. Rev. A **82**, 012116 (2010).

[40] J. J. Halliwell, E. Gillman, O. Lennon, M. Patel, and I. Ramirez, Quantum backflow states from eigenstates of the regularized current operator, J. Phys. A: Math. Theor. **46**, 475303 (2013).

[41] C. R. Greenshields, R. L. Stamps, S. Franke-Arnold, and S. M. Barnett, Is the Angular Momentum of an Electron Conserved in a Uniform Magnetic Field? Phys. Rev. Lett. **113**, 240404 (2014).

[42] B. Berche, D. Malterre, and E. Medina, Gauge transformations and conserved quantities in classical and quantum mechanics, Am. J. Phys. **84**, 616 (2016).

[43] M. Wakamatsu, Y. Kitadono, and P.-M. Zhang, The issue of gauge choice in the Landau problem and the physics of canonical and mechanical orbital angular momenta, Ann. Phys. **392**, 287 (2018).

[44] Y. Kitadono, A test of gauge invariant canonical angular momentum in Landau level problem, in *Proceedings of the 8th International Conference on Quarks and Nuclear Physics (QNP2018), November 13-17, 2018, Tsukuba, Ibaraki, Japan* (Physical Society of Japan, Japan, 2018).